The EMBO Journal (2012) 31, 2156–2168 | © 2012 European Molecular Biology Organization | All Rights Reserved 0261-4189/12
www.embojournal.org

THE EMBO JOURNAL

Munc18-1 mutations that strongly impair SNARE-complex binding support normal synaptic transmission

Marieke Meijer[1,4], Pawel Burkhardt[2,4,5], Heidi de Wit[1], Ruud F Toonen[1], Dirk Fasshauer[2,3,*] and Matthijs Verhage[1,*]

[1]Department of Functional Genomics and Department of Clinical Genetics, Center for Neurogenomics and Cognitive Research, Neuroscience Campus Amsterdam, VU University Amsterdam and VU University Medical Center, Amsterdam, The Netherlands, [2]Research Group Structural Biochemistry, Department of Neurobiology, Max-Planck-Institute for Biophysical Chemistry, (MPIbpc), Göttingen, Germany and [3]Department of Cellular Biology and Morphology, University of Lausanne, Lausanne, Switzerland

Synaptic transmission depends critically on the Sec1p/Munc18 protein Munc18-1, but it is unclear whether Munc18-1 primarily operates as a integral part of the fusion machinery or has a more upstream role in fusion complex assembly. Here, we show that point mutations in Munc18-1 that interfere with binding to the free Syntaxin1a N-terminus and strongly impair binding to assembled SNARE complexes all support normal docking, priming and fusion of synaptic vesicles, and normal synaptic plasticity in *munc18-1* null mutant neurons. These data support a prevailing role of Munc18-1 before/during SNARE-complex assembly, while its continued association to assembled SNARE complexes is dispensable for synaptic transmission.

The EMBO Journal (2012) **31,** 2156–2168. doi:10.1038/emboj.2012.72; Published online 23 March 2012
Subject Categories: membranes & transport; neuroscience
Keywords: exocytosis; Munc18-1; SM proteins; SNARE complex; Syntaxin1a

Introduction

Synaptic vesicle exocytosis is executed by a multi-subunit protein machinery between vesicle and target membrane. The central components of the machinery are the SNARE proteins Syntaxin1, SNAP25 and Synaptobrevin2/VAMP2. In preparation for the final fusion event, the exocytotic machinery goes through several molecular steps involving conformational changes and association/dissociation of additional factors. Due to the fact that individual components are integral parts of the machinery, it has proven difficult to assign a precise role for each component and to determine the precise course of events.

One key factor for which it has been difficult to define the precise role in neuronal secretion is the Sec1p/Munc18 (SM) protein Munc18-1 (Toonen and Verhage, 2003; Toonen and Verhage, 2007; Burgoyne *et al*, 2009; Sudhof and Rothman, 2009; Carr and Rizo, 2010; Han *et al*, 2010; Smyth *et al*, 2010). Deletion of Munc18-1 in mice leads to the complete loss of neurotransmitter secretion (Verhage *et al*, 2000), and similar results have been found in *Caenorhabditis elegans* and *Drosophila melanogaster* (Harrison *et al*, 1994; Weimer *et al*, 2003). Based on *in vivo* studies, Munc18-1 is thought to be involved in the initial docking step (Voets *et al*, 2001; Weimer *et al*, 2003; Toonen *et al*, 2006a; de Wit *et al*, 2009) but also has a post-docking role (Gulyas-Kovacs *et al*, 2007; de Wit *et al*, 2009), and is proposed to promote/regulate the final fusion reaction (Fisher *et al*, 2001; Graham *et al*, 2004; Jorgacevski *et al*, 2011). However, other studies suggest that Munc18-1 is no longer required as an integral part of the fusion machinery once the SNARE complex is formed (Zilly *et al*, 2006; Rathore *et al*, 2010).

Comparably, biochemical investigations on the interaction of Munc18-1 with the core SNARE machinery have provided data that are difficult to reconcile. Indisputable, however, is that Munc18-1 binds tightly to monomer Syntaxin1. Interestingly, this interaction involves two sites on opposing surfaces of Munc18-1, which bind to the far N-terminal end of Syntaxin (N-peptide) and the remainder of the protein in closed conformation (Misura *et al*, 2000; Burkhardt *et al*, 2008). In this configuration, Munc18-1 prevents Syntaxin1 from participating in SNARE complex formation (Pevsner *et al*, 1994a; Yang *et al*, 2000; Rickman *et al*, 2007; Brandie *et al*, 2008; Burkhardt *et al*, 2008). At first sight, this inhibitory activity appears to be inconsistent with the null mutant phenotype (Verhage *et al*, 2000). However, when the N-peptide of Syntaxin cannot bind, Munc18-1-bound Syntaxin1 can readily assemble into SNARE complexes (Burkhardt *et al*, 2008). This indicates that Munc18-1 is able to guide Syntaxin towards productive SNARE complex formation and reveals that both binding sites act together. Remarkably, a similar structure with similar functionality has recently been uncovered for the homologous Munc18/Syntaxin 1 complex of the choanoflagellate *Monosiga brevicollis* (Burkhardt *et al*, 2011). Choanoflagellates are the closest living unicellular relatives of animals, suggesting that the neuronal Munc18-1/Syntaxin1 complex is evolutionary highly conserved.

On the other hand, based mainly on insights gained upon studying the yeast ortholog Sec1p, it was suggested that SM

*Corresponding author. D Fasshauer, Research Group Structural Biochemistry, Department of Neurobiology, Max-Planck-Institute for Biophysical Chemistry, (MPIbpc), Am Fassberg 11, Göttingen 37077, Germany. Tel.: +41 21 6925287; Fax: +41 21 6925105;
E-mail: Dirk.Fasshauer@unil.ch or M Verhage, Department of Functional Genomics and Department of Clinical Genetics, Center for Neurogenomics and Cognitive Research, Neuroscience Campus Amsterdam, VU University Amsterdam and VU University Medical Center, De Boelelaan 1085, 1081 HV, Amsterdam, The Netherlands. Tel.: +31 20 5986936; Fax: +31 20 5986926;
E-mail: matthijs.verhage@cncr.vu.nl
[4]These authors contributed equally to this work
[5]Present address: Department of Molecular and Cell Biology, University of California at Berkeley, Berkeley, CA 94720, USA

Received: 11 January 2012; accepted: 28 February 2012; published online 23 March 2012

proteins might function as part of the core vesicle fusion machinery, promoting fusion when bound to the assembled SNARE complex (Carr *et al*, 1999; Scott *et al*, 2004; Togneri *et al*, 2006). Whether or not Munc18-1 behaves like Sec1p and primarily acts as part of the assembled SNARE complexes has been a matter of intense debate. Indeed, this mode of action of Munc18 appears to be supported by biochemical experiments that show that Munc18-1 binds to assembled SNARE complexes via the N-peptide of Syntaxin, although with much lower affinity compared to monomeric Syntaxin (Hata *et al*, 1993; Pevsner *et al*, 1994b; Dulubova *et al*, 1999; Misura *et al*, 2000; Dulubova *et al*, 2007; Khvotchev *et al*, 2007; Rickman *et al*, 2007; Shen *et al*, 2007; Burkhardt *et al*, 2008; Guan *et al*, 2008; Rodkey *et al*, 2008; Weninger *et al*, 2008), and with even lower affinity (although still in the sub-micromolar range) to vesicle SNAREs or the core SNARE complex (Xu *et al*, 2010). Moreover, a number of recent studies reported an accelerating effect of Munc18-1 in a liposome fusion assay (Shen *et al*, 2007; Rodkey *et al*, 2008; Diao *et al*, 2010; Shen *et al*, 2010; Schollmeier *et al*, 2011).

One strategy to discriminate between action of Munc18-1 on assembled SNARE complexes or a role in more upstream events has been to introduce point mutations that interfere with binding to assembled SNARE complexes while preserving affinity for Syntaxin1 in its closed conformation (Misura *et al*, 2000). Several mutations in Munc18 have been described, designed to interfere either with the N-peptide or the N-terminal three-helix-bundle of Syntaxin (the Habc domain). Since the interaction of Munc18-1 with assembled SNARE complexes strongly depends on the N-peptide, at least *in vitro* (Dulubova *et al*, 2007; Shen *et al*, 2007; Burkhardt *et al*, 2008), such mutations might be instrumental to address the biological relevance of SNARE-complex binding. Mutations interfering with N-peptide binding were indeed not able to rescue the function of the nematode ortholog, UNC-18 (McEwen and Kaplan, 2008; Johnson *et al*, 2009), although similar mutations in Munc18-1 had a moderate effect upon overexpression in PC12 cells (Malintan *et al*, 2009). Moreover, mutations in the N-peptide of Syntaxin produced strong inhibition of secretion in nematodes and disrupted the accelerating effect of Munc18-1 on liposome fusion (Shen *et al*, 2007; Johnson *et al*, 2009; Rathore *et al*, 2010; Schollmeier *et al*, 2011).

Here, we combine quantitative biochemistry with synapse physiology and electron microscopy in mammalian neurons on a null mutant background to dissect Munc18-1's function on assembled SNARE complexes and in more upstream functions. We generated two Munc18-1 mutations that inhibit binding to the Syntaxin N-peptide and a third, previously published mutation (Deak *et al*, 2009), which affects SNARE-complex interaction by disrupting the interaction with the Syntaxin Habc domain. As a result, these mutants have no detectable affinity for assembled SNARE complexes. Surprisingly, these mutants support synaptic transmission equally well as wild-type Munc18-1. Our data are inconsistent with the proposed role of Munc18-1 in promoting fusion via binding to assembled SNARE complexes. Instead, we propose a model in which Munc18-1 assists primarily in setting up SNARE complexes, while downstream association with fusion complexes is dispensable.

Results

Munc18-1 mutations in the N-peptide-binding pocket reduce affinity for SNARE complexes

To study the relevance for synaptic transmission of Munc18-1 binding to the N-peptide of Syntaxin and thereby to assembled SNARE complexes, we generated a new mutant inspired by $Sly1p_{L140K}$ (Peng and Gallwitz, 2004), which interferes with the hydrophobic nature of the N-peptide-binding pocket ($M18_{L130K}$, Figure 1A). Using isothermal titration calorimetry (ITC), we previously showed that Munc18-1 binds assembled SNARE complexes with relatively low affinity, and that there is no detectable interaction if the SNARE complex contains a N-terminally truncated Syntaxin1a (Burkhardt *et al*, 2008). As expected, for $M18_{L130K}$ no binding to assembled SNARE complexes could be detected by our ITC measurement (Figure 1B; Table I). Since the N-peptide attributes to the affinity of Munc18-1 for monomeric Syntaxin1a, $M18_{L130K}$ showed also reduced affinity and enthalpy for $Syx1a_{1-262}$ (Figure 1C; Table I). Truncating the N-terminus of Syntaxin1a did not reduce the affinity further, supporting the notion that the reduced affinity is caused by disrupted N-peptide binding (Figure 1D; Table I). The reduced affinity for monomeric Syntaxin1a can be mainly attributed to an increased off-rate of the $M18\text{-}1_{L130K}$/Syx1a complex (Figure 1E), which was about 10 times higher than for $M18_{WT}$ ($M18_{WT} \approx 0.0011\ s^{-1}$, $M18_{L130K} \approx 0.010\ s^{-1}$).

SNARE complex formation is blocked when the Syntaxin1a N-peptide is bound to Munc18-1 (Burkhardt *et al*, 2008). To test if $M18_{L130K}$ was still able to block ternary SNARE-complex formation, we used a fluorescence-based SNARE-binding assay. When the labelled cytosolic domain of $Syb2_{1-96}$ was mixed with $Syx1a_{1-262}$ and SNAP25, the fluorescence anisotropy increased, indicating SNARE-complex formation (Figure 1F). $M18_{L130K}$ still inhibited, or at least slowed down considerably, SNARE-complex formation, but inhibition was not as complete as for $M18_{WT}$ (Figure 1F). Taken together, these biochemical assays confirm that interfering with N-peptide binding strongly impairs binding of Munc18-1 to the SNARE complex. In addition, the results reveal that $M18_{L130K}$ is much less efficient in inhibiting SNARE-complex formation than $M18_{WT}$, highlighting again the crucial role of the N-peptide-binding site for the inhibitory role of Munc18 on SNARE-complex formation.

Neurons expressing an N-peptide-binding mutant show normal survival and vesicle docking

As the first step in analysing the relevance of N-peptide and SNARE-complex binding for synaptic transmission, we studied docking in autaptic *munc18-1* null mutant neurons rescued with either $M18_{WT}$ or $M18_{L130K}$. Neurons rescued with $M18_{WT}$ or $M18_{L130K}$ survived and developed with similar morphology and synapse density (Supplementary Figure S2A–D). As Munc18-1 expression level controls the number of docked vesicles and presynaptic output (Toonen *et al*, 2006b), we analysed synaptic Munc18-1 expression using semiquantitative immuno-fluorescence detection in VAMP2-positive synapses using an automated image analysis routine (Schmitz *et al*, 2011). Synaptic $M18_{L130K}$ levels were equal to $M18_{WT}$ (Supplementary Figure S2E). Docking of synaptic vesicles at the active zone and other ultrastructural features

of the synapse were analysed by electron microscopy (Figure 1G and H). The number of docked vesicles in neurons rescued with $M18_{L130K}$ was similar to $M18_{WT}$ (Figure 1H). We used classical chemical fixation of these neurons, which might, together with the definition of 'docking' (see discussion in (Verhage and Sorensen, 2008)), produce a different absolute number of docked vesicles than when using rapid freeze fixation and/or other docking definitions, but this is unlikely to affect relative differences between experimental groups. The total number of vesicles and the amount of docked vesicles per nm active zone, as well as the size of the active zone and postsynaptic density did not differ between groups, confirming unchanged synaptic morphology (Figure 1H and Supplementary Figure S3A–B).

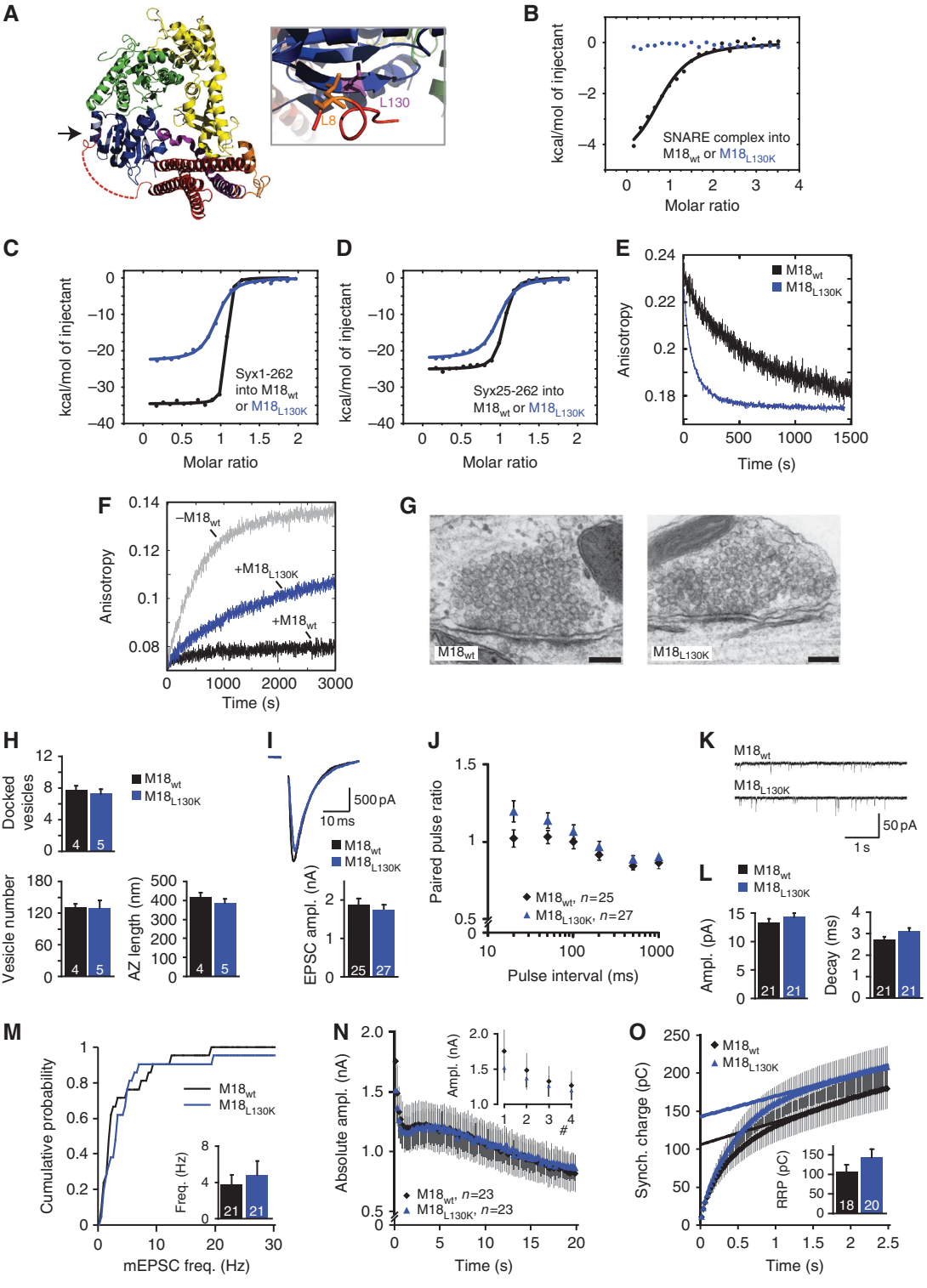

Synaptic transmission is unaffected by disrupted N-peptide and SNARE binding

As the second step, we studied priming and fusion in null mutant neurons rescued with either $M18_{WT}$ or $M18_{L130K}$. Neurons rescued with $M18_{L130K}$ produced excitatory postsynaptic currents (EPSCs) upon depolarization that were similar to neurons rescued with $M18_{WT}$ (Figure 1I). The ratio between synaptic responses to two subsequent stimuli given at various time intervals (paired-pulse ratio; PPR) is a measure for release probability (Pr). The PPRs were also similar between neurons rescued with $M18_{WT}$ and $M18_{L130K}$ (Figure 1J). Furthermore, spontaneous release of single vesicles (miniature EPSCs) occurred at similar rate, and quantal size and mEPSC kinetics were similar (Figure 1K–M).

Changes in release efficiency or refilling might become evident when stimulation is continued for longer periods. However, neurons rescued with $M18_{L130K}$ displayed normal depression of EPSC size during stimulation trains at 5, 10 or 40 Hz (Figure 1N and Supplementary Figure S4A–B). In addition, RRP estimates derived by back-extrapolation from the cumulative synchronous charge released during a 40-Hz train indicated that the RRP was unaffected (Figure 1O) (Schneggenburger *et al*, 1999). Since synaptic release shifts from synchronous to asynchronous release during and after intense stimulation, a 40-Hz train can be used to monitor changes in synchronicity. Neurons rescued with $M18_{L130K}$ showed a similar pattern (synchronous charge/total charge) to neurons rescued with $M18_{WT}$ (Supplementary Figure S4C). To conclude, our data show that interfering with binding of Munc18-1 to the N-peptide of Syntaxin1 does not have a detectable effect on synaptic transmission in autaptic hippocampal neurons using our assays.

Table I Thermodynamic parameters of the interaction of Syntaxin1a and Munc18-1 measured by ITC

Interaction of	K_d (nM)	ΔH° (kcal/mol)	n
$Syx1a_{1-262}/M18_{wt}$[a]	1.4 ± 0.3	− 34.6 ± 0.2	1.03
$Syx1a_{1-262}/M18_{L130K}$	28.2 ± 3.7	− 22.7 ± 0.3	0.91
$Syx1a_{1-262}/M18_{F115E}$	6.6 ± 1.4	− 25.8 ± 0.2	0.91
$Syx1a_{1-262}/M18_{E59K}$	48.1 ± 5.6	− 14.7 ± 0.2	0.98
$Syx1a_{25-262}/M18_{wt}$[a]	8.1 ± 1.0	− 25.1 ± 0.2	1.01
$Syx1a_{25-262}/M18_{L130K}$	30.4 ± 3.6	− 22.1 ± 0.2	0.95
$Syx1a_{25-262}/M18_{F115E}$	19.2 ± 6.4	− 25.1 ± 0.6	0.98
SNARE complex with $Syx1a_{1-262}/M18_{wt}$[a]	719.4 ± 118.0	− 4.8 ± 0.4	0.84
SNARE complex with $Syx1a_{1-262}/M18_{L130K}$	—	—	—
SNARE complex with $Syx1a_{1-262}/M18_{F115E}$	—	—	—
SNARE complex with $Syx1a_{1-262}/M18_{E59K}$	—	—	—
SNARE complex with $Syx1a_{25-262}/M18_{wt}$	—	—	—

The experimental isothermal titration calorimetry (ITC) data for the interaction of Syntaxin1a and Munc18-1 variants are shown in Supplementary Figure 1. The errors reported in Table I are the numbers obtained from fitting the data of a single ITC run.
[a]From Burkhardt *et al*, 2008.

A second N-peptide mutant behaves like L130K in biochemical, electron microscopic and electrophysiological analyses

For comparison, we studied a second N-peptide-binding pocket mutant, $M18_{F115E}$ (Figure 2A). This mutant was inspired by published mutations in Sly1p and Munc18c, which severely impaired binding to the N-terminus of their cognate Syntaxins, Syntaxin4 and Sed5p, respectively (Peng and Gallwitz, 2004; Latham *et al*, 2006), and was recently also generated in Munc18-1 (Malintan *et al*, 2009). This mutation provides a second, independent approach for analysing the relevance of N-peptide and SNARE-complex binding within the N-peptide-binding pocket. Like for $M18_{L130K}$, we found that $M18_{F115E}$ does not bind to the assembled SNARE complex using ITC (Figure 2B; Table I), consistent with previous co-precipitation data (Malintan *et al*, 2009). In addition, $M18_{F115E}$ showed reduced enthalpy and affinity for monomeric Syntaxin1a, and the enthalpy was not lowered further by additional removal of the N-peptide (Figure 2C and D). $M18_{F115E}$ behaved also very similar to $M18_{L130K}$ in Syx1a dissociation and SNARE-formation assays as it showed a faster dissociation rate constant ($M18_{F115E} \approx 0.0085\ s^{-1}$) and a reduced ability to inhibit SNARE-complex formation (Figure 2E and F).

Munc18-1 null neurons could also be rescued with $M18_{F115E}$ in autaptic culture. Again, overall morphology and synapse density of rescued neurons was not different between neurons rescued with $M18_{WT}$ and $M18_{F115E}$ (Supplementary Figure S2A–D). Unexpectedly, synaptic Munc18-1 levels were higher than in neurons rescued with $M18_{WT}$ or $M18_{L130K}$ (Supplementary Figure S2E). Reducing

Figure 1 Mutation in the N-peptide-binding pocket that disrupts SNARE-complex binding supports normal synaptic transmission. (**A**) Crystal structure of the M18-1/Syx1a complex represented as ribbon (left), with Munc18-1 in blue–green–yellow and Syx1a in purple–orange–red (adapted from Misura *et al*, 2000; Burkhardt *et al*, 2008). Arrow is pointing to the N-peptide-binding pocket. Close-up of the N-peptide-binding pocket with the residue targeted for mutagenesis in purple and the key residue of the Syntaxin1a N-peptide in orange (right). (**B**) Titration of the neuronal SNARE complex containing $Syx1a_{1-262}$ into $M18_{WT}$ (black curve) or $M18_{L130K}$ (blue curve). Shown are the integrated areas normalized to the amount of SNARE complex injected (kcal/mol) versus its molar ratio to Munc18-1. (**C**) Calorimetric titrations of monomer $Syx1a_{1-262}$ into Munc18-1. (**D**) Calorimetric titrations of monomer $Syx1a_{25-262}$ into Munc18-1. (**E**) Determination of the off-rate of the Munc18-1/Syntaxin1a complex by competitive dissociation ($M18_{WT} \approx 0.0011\ s^{-1}$ (from Burkhardt *et al*, 2008), black curve; $M18_{L130K} \approx 0.010\ s^{-1}$, blue curve). (**F**) Ternary SNARE-complex formation was followed in the absence (grey curve) or presence of Munc18-1 ($M18_{WT}$, black; $M18_{L130K}$, blue). (**G**) Electron micrographs of typical asymmetrical glutamatergic synapses from neurons rescued with $M18\text{-}1_{WT}$ or $M18\text{-}1_{L130K}$. Scale bar = 100 nm. (**H**) Neurons rescued with $M18\text{-}1_{L130K}$ have a normal SV docking and a normal ultrastructure. $N = 4–5$ islands, $n = 98–102$ synapses. (**I**) Autaptic neurons rescued with $M18_{L130K}$ have similar EPSC sizes as neurons rescued with $M18_{WT}$. Upper panel shows typical EPSC traces (artifacts removed). (**J**) No differences were found in PPRs (second EPSC/first EPSC). (**K**) Example traces of spontaneous release in autaptic neurons. (**L**) Spontaneous release amplitude and decay time are comparable. (**M**) Cumulative frequency plot of spontaneous release events. Insert shows average frequency. (**N**) Depression of EPSC size during repetitive stimulation at 5 Hz is normal. Inset shows the first four pulses. (**O**) An estimate of RRP size was made by back-extrapolation from the cumulative synchronous charge from the last 40 pulses within a 100-pulse train at 40 Hz. No differences in RRP size were found.

infection titres could not reduce cellular levels of $M18_{F115E}$ without compromising rescue efficiency/survival. Hence, $M18_{F115E}$, unlike $M18_{L130K}$ (and $M18_{E59K}$, see below), can be considered as an over-expression model and allows answering the question whether higher levels of interfering mutations might inhibit SNARE-complex formation, alter synaptic transmission and produce different phenotypes.

Despite higher synaptic levels, the number of docked vesicles was similar between neurons rescued with $M18_{F115E}$ or $M18_{WT}$ (Figure 2G and H) and therefore also

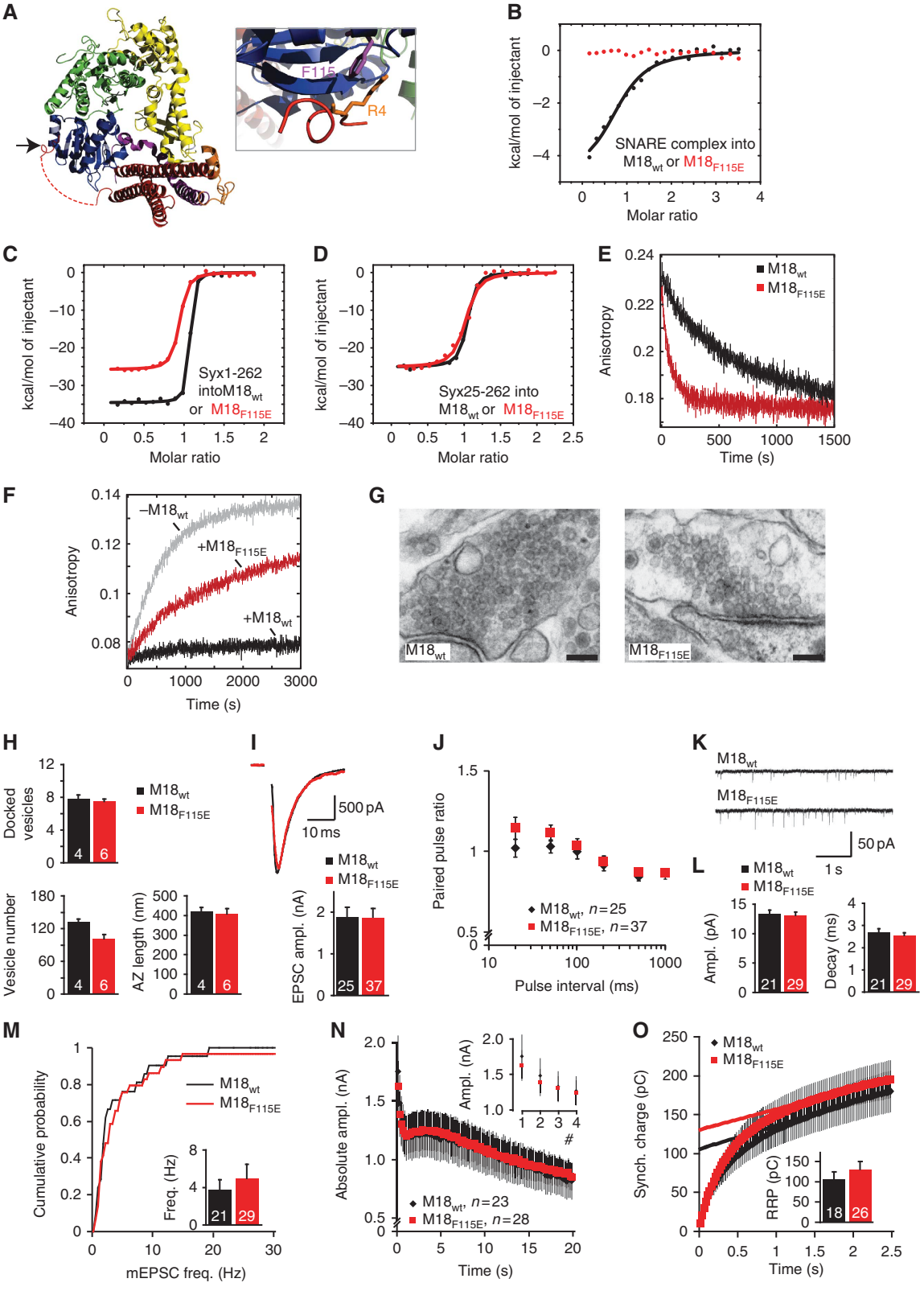

similar to M18-1_{L130K} (Figure 1G and H). The total number of vesicles, size of the active zone and other morphometric parameters all did not differ between null mutant neurons rescued with $M18_{WT}$ or $M18_{F115E}$ (Figure 2G and H and Supplementary Figure S3). Overexpression (Supplementary Figure S2E) is not as high as with Semliki Forest viral infection that we previously used to produce the highest cellular Munc18-1 levels (Toonen *et al*, 2006b), and the lack of ultrastructural effects of higher cellular Munc18-1 levels are consistent with earlier findings (Toonen *et al*, 2006b). EPSC sizes were also identical between neurons rescued with $M18_{WT}$ and $M18_{F115E}$ as were PPRs, indicating a normal Pr (Figure 2I and J). Spontaneous release was also normal in event frequency, size and kinetics (Figure 2K–M). EPSCs obtained by a train of stimulation at 5, 10 or 40 Hz followed a normal decline of amplitude and shift from synchronous to asynchronous release (Figure 2N and Supplementary Figure S4D–F). In addition, RRP estimates derived by back-extrapolation from the cumulative synchronous charge released during a 40-Hz train indicated a normal RRP size in neurons rescued with $M18_{F115E}$ (Figure 2O). Together, these results show that another point mutation within the N-peptide-binding pocket, $M18_{F115E}$, behaves identically to $M18_{L130K}$ in biochemical assays and electrophysiological measurements. This further supports our hypothesis that N-peptide and SNARE-complex binding are not required for normal synaptic transmission.

A mutant that disrupts SNARE binding also supports normal synaptic transmission

Munc18-1 has been reported to control synaptic vesicle priming via interactions with the assembled SNARE complex. A mutation, $M18_{E59K}$, has been introduced in the N-terminal domain of Munc18-1, which contacts the Syntaxin Habc domain (Figure 3A) and was previously characterized to disrupt binding to the SNARE complex while leaving the N-peptide-binding pocket intact. Compound EPSCs and spontaneous release frequency were severely reduced in network cultures of neurons expressing this mutant (Deak *et al*, 2009). Since our findings do not support a critical role for Munc18-1 at the assembled SNARE complex in synaptic transmission, we also tested $M18_{E59K}$ in our autaptic cultures. Our ITC measurements confirmed that $M18_{E59K}$ lowered the affinity for SNARE complexes beyond detection (Figure 3B; Table I). $M18_{E59K}$ also exhibited a lower affinity than $M18_{WT}$ for monomer Syntaxin1a (Kd $\approx$ 48.1 nM, Figure 3C; Table I). Notably, the affinity determined by us is somewhat lower than what has been reported originally (12 nM, (Deak *et al*, 2009)). In this study, the affinity for the wild-type interaction was determined to be $\approx$7.5 nM, which suggested that the E59K mutation only slightly affected the interaction with the closed conformation of Syntaxin1a. By contrast, our data, in agreement with a recent study (Han *et al*, 2011), reveal that the affinity is more strongly affected by the point mutation. The reduced overall affinity for Syntaxin1a is probably caused by a faster rate of dissociation ($k_{off} \approx 0.072\ s^{-1}$) (Figure 3D), a feature not previously documented. Also, we found that $M18_{E59K}$ completely lost the ability to inhibit SNARE-complex formation, which occurred at about similar speed as in the absence of Munc18-1 (Figure 3E).

We then expressed $M18_{E59K}$ in autaptic hippocampal *munc18-1* null neurons. Neurons rescued with $M18_{E59K}$ had a similar morphology and synapse density as neurons rescued with $M18_{WT}$ (Supplementary Figure S2A–D). However, synaptic Munc18-1 levels were lower (Supplementary Figure S2E–F). This could not be normalized by increasing viral load and might be due to decreased protein stability upon introduction of the mutation (as also noticed previously (Deak *et al*, 2009)). Under these conditions, ultrastructural analyses on rescued neurons showed that neurons rescued with $M18_{E59K}$ were capable of docking synaptic vesicles and have a total number of vesicles and ultrastructural features comparable to neurons expressing $M18_{WT}$ (Figure 3F and G and Supplementary Figure S3).

Nonetheless, neurons rescued with $M18_{E59K}$ showed normal EPSC sizes (Figure 3H), confirming that the interaction between Munc18-1 and the SNARE complex is not essential for synaptic transmission. However, we observed that a smaller number of neurons responded to stimulation, resulting in a higher number of cells being excluded from analysis (see Materials and methods). The average synaptic $M18_{E59K}$ levels per neuron varied widely, and despite the lower average $M18_{E59K}$ level, some neurons did express higher levels (Supplementary Figure S2F). It is conceivable that neurotransmission in these neurons is normal, while in low-expressing neurons neurotransmission is abolished. Responsive neurons expressing $M18_{E59K}$ displayed an

Figure 2 A second mutation in the N-peptide-binding pocket that disrupts SNARE-complex binding also supports normal synaptic transmission. (**A**) Crystal structure of the M18-1/Syx1a complex represented as ribbon (left), with Munc18-1 in blue–green–yellow and Syx1a in purple–orange–red (adapted from Misura *et al*, 2000; Burkhardt *et al*, 2008). Arrow is pointing to the N-peptide-binding pocket. A close-up of the N-peptide-binding pocket with the residue targeted for mutagenesis in purple and the key residue of the Syntaxin1a N-peptide in orange (right). (**B**) Titration of the neuronal SNARE complex containing $Syx1a_{1-262}$ into $M18_{WT}$ (black curve) or $M18_{F115E}$ (red curve). Shown are the integrated areas normalized to the amount of SNARE complex injected (kcal/mol) versus its molar ratio to Munc18-1. (**C**) Calorimetric titrations of monomer $Syx1a_{1-262}$ into Munc18-1. (**D**) Calorimetric titrations of $Syx1a_{25-262}$ into Munc18-1. (**E**) Determination of the off-rate of the Munc18-1/Syntaxin1a complex by competitive dissociation ($M18_{WT} \approx 0.0011\ s^{-1}$ (from Burkhardt *et al*, 2008), black curve; $M18_{F115E} \approx 0.0085\ s^{-1}$, red curve). (**F**) Ternary SNARE-complex formation was followed in the absence (grey curve) or presence of Munc18-1 ($M18_{WT}$, black; $M18_{F115E}$, red). (**G**) Electron micrographs of typical asymmetrical glutamatergic synapses from neurons rescued with M18-1_{WT} or M18-1_{F115E}. Scale bar = 100 nm. (**H**) Neurons rescued with M18-1_{F115E} have normal numbers of vesicles docked at the active zone and in total. Active zone size is normal. $N = 4$–6 islands, $n = 98$–100 synapses. (**I**) Autaptic neurons rescued with $M18_{F115E}$ have similar EPSC sizes as neurons rescued with $M18_{WT}$. Upper panel shows typical EPSC traces (artifacts removed). (**J**) No differences were found in PPRs (second EPSC/first EPSC). (**K**) Example traces of spontaneous release in autaptic neurons. (**L**) Spontaneous release amplitude and decay time are comparable. (**M**) Cumulative frequency plot of spontaneous release events. Insert shows average frequency. (**N**) Depression of EPSC size during repetitive stimulation at 5 Hz is normal. Inset shows first four pulses. (**O**) An estimate of RRP size was made by back-extrapolation from the cumulative synchronous charge from the last 40 pulses within a 100-pulse train at 40 Hz. Inset shows average RRP sizes. No differences in RRP size were found.

enhanced PPR at the 20-ms inter-pulse interval (Figure 3I), suggesting a decreased initial Pr. Spontaneous release frequency was unchanged in neurons rescued with $M18_{E59K}$ but the average mEPSC amplitude was slightly lower (Figure 3J–L). Stimulation at 10 and 40 Hz resulted in normal run-down of EPSCs (Figure 3M and Supplementary Figure S4G). RRP estimates derived from 40-Hz stimulation trains are not significantly different from neurons rescued with $M18_{WT}$ (Figure 3N), nor is the shift in synchronicity in these trains (Supplementary Figure S4H).

Since the initial hypothesis that Munc18-1 controls synaptic vesicle priming via interactions with the SNARE complex originated from data obtained in network cultures (Deak *et al*, 2009), we also tested all three mutants in network

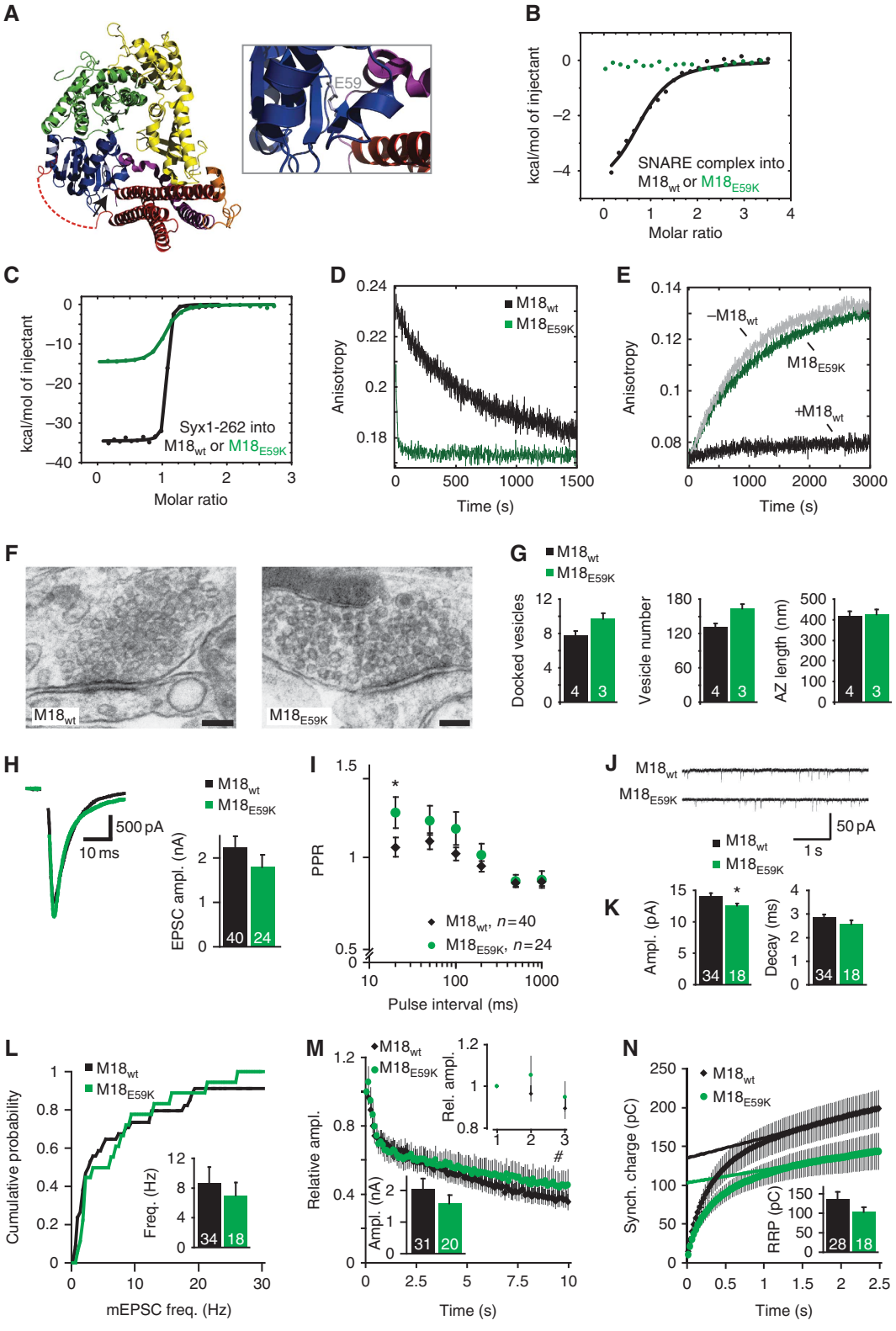

cultures (Supplementary Figure S5). Networks of cortical neurons rescued with $M18_{E59K}$ responded with smaller peak amplitudes to local field stimulation (Supplementary Figure S5G), consistent with previous data (Deak *et al*, 2009). The high proportion of nonresponding neurons as found in autaptic cultures (>60%) provides a likely explanation for this reduced average response in mass culture. As in autaptic cultures, network cultures rescued with the N-peptide mutants $M18_{L130K}$ and $M18_{F115E}$ supported synaptic transmission and responded to field stimulation with similar peak amplitudes as cultures rescued with $M18_{WT}$ (Supplementary Figure S5A–F). However, interpretation of network cultures is more complex compared to autaptic cultures due to confounding factors like cell density and homoeostatic plasticity, especially when cell survival depends on efficient protein expression as is the case here.

Discussion

In this study, we tested the concept that binding of Munc18-1 to assembled SNARE complexes via the N-terminus is an important aspect of Munc18-1's role in synaptic transmission. We tested this *in situ*, by analysing synaptic transmission in living neurons from *munc18-1* null mutant mice. In these 'rescued' neurons, synapses depend solely on Munc18-1 carrying a mutation that interferes with binding to the N-peptide of Syntaxin and strongly impairs binding to the assembled SNARE complex. Using this system, we found no support for the concept that Munc18-1 promotes fusion efficiency by binding to SNARE complexes. The Munc18-1 mutations that lost affinity for assembled SNARE complexes support synaptic transmission equally well as $M18_{WT}$. Hence, while binding assembled SNARE complexes and thereby promoting fusion may be a central aspect of some SM proteins (Carr *et al*, 1999; Scott *et al*, 2004; Togneri *et al*, 2006; McEwen and Kaplan, 2008; Hashizume *et al*, 2009; Johnson *et al*, 2009; Pieren *et al*, 2010), this is probably not a universal feature of all SM proteins.

The idea that SM proteins primarily act on assembled SNARE complexes was originally proposed on the basis of studies on the yeast SM protein involved in plasma membrane fusion, Sec1p. Sec1p has been shown to be unable to bind its cognate Syntaxin, Sso1p, but is thought to interact primarily with the assembled ternary SNARE complex (Carr *et al*, 1999; Scott *et al*, 2004; Togneri *et al*, 2006; Hashizume *et al*, 2009). The recently determined structure of the primordial Munc18/Syntaxin 1 complex of the choanoflagellate *M. brevicollis* suggests, however, that not the neuronal Munc18-1/Syntaxin complex but rather yeast Sec1p is deviated. In fact, the secretory Syntaxin of yeast, Sso1p, in contrast to most other eukaryotic lineages, seems to have lost a canonical N-terminal peptide sequence, suggesting that the mode of its interaction with the SNARE machinery diverged during fungal evolution. Moreover, a recent study shows that Sec1p contains a unique C-terminal tail, which preferentially binds SNARE complexes and is absent in other SM proteins (Weber-Boyvat *et al*, 2011). Furthermore, several additional actions of Sec1p have been characterized, suggesting that Sec1p also has more upstream actions potentially similar to those of Munc18-1 (Hashizume *et al*, 2009).

The fact that SNARE-complex binding is not crucial for synaptic transmission in mammalian neurons might be considered an evolutionary adaptation. However, disrupting the N-peptide interaction between two other SM proteins, Sly1p or Vsp45p, and their cognate Syntaxins also had no functional impact (Peng and Gallwitz, 2004; Carpp *et al*, 2006), suggesting that actions on assembled SNARE complexes might already vary among different SM proteins. The lack of effect of N-peptide mutations on synaptic transmission (and other fusion events in the cell) might in principle also be an additive effect of two separate effects, one being inhibited and one being stimulated by loss of N-peptide binding. However, the different functional assays used in this study are expected to unmask such dual, opposite effects, since these assays probe different aspects of Munc18-1 function to a different extent. For example, morphological docking analysis and RRP estimates probe specifically the more upstream actions of Munc18-1 and should report changes if the overall lack of effect on synaptic transmission would result from an additive effect of two underlying opposite effects of N-peptide mutations.

While in agreement with studies on yeast Sly1p and Vsp45p listed above, our findings contrast somewhat with several others. First, *C. elegans* UNC-18 binding to the N-peptide of Syntaxin/UNC-64 is required for synaptic function (McEwen and Kaplan, 2008; Johnson *et al*, 2009). Second, Syntaxin N-peptide injected or overexpressed in different systems inhibits fusion (Yamaguchi *et al*, 2002; Dulubova *et al*, 2003; Williams *et al*, 2004) including mammalian neurotransmitter secretion (Khvotchev *et al*, 2007). It is conceivable that the N-peptide fragment interferes with fusion in these systems irrespective of SM protein binding to the SNARE complex, or that the N-peptide

Figure 3 A subpopulation of $M18_{E59K}$ expressing neurons support neurotransmission. (**A**) Crystal structure of the M18-1/Syx1a complex represented as ribbon (left), with Munc18-1 in blue–green–yellow and Syx1a in purple–orange–red (adapted from Misura *et al*, 2000; Burkhardt *et al*, 2008). Arrow is pointing to the site of mutagenesis. Close-up of the E59 residue in grey (right). (**B**) Titration of the neuronal SNARE complex containing $Syx1a_{1-262}$ into Munc18-1. (**C**) Titration of monomer $Syx1a_{1-262}$ into Munc18-1. (**D**) Determination of the off-rate of the Munc18-1/Syntaxin1a complex by competitive dissociation ($M18_{WT} \approx 0.0011\ s^{-1}$ (from Burkhardt *et al*, 2008), black curve; $M18_{E59K} \approx 0.072\ s^{-1}$, green curve). (**E**) Ternary SNARE-complex formation was followed in the absence (grey curve) or presence of Munc18-1 ($M18_{WT}$, black; $M18_{E59K}$, green). (**F**) Electron micrographs of typical asymmetrical glutamatergic synapses from neurons rescued with $M18\text{-}1_{WT}$ or $M18\text{-}1_{E59K}$. Scale bar = 100 nm. (**G**) Neurons rescued with $M18\text{-}1_{E59K}$ are capable of docking synaptic vesicles. Active zone size is normal. $N = 3$–4 islands, $n = 85$–98 synapses. (**H**) Autaptic neurons rescued with $M18_{E59K}$ have similar EPSC sizes as neurons rescued with $M18_{WT}$. Left panel shows typical EPSC traces (artifacts removed). (**I**) PPR was increased at the 20-ms pulse interval in neurons rescued with $M18_{E59K}$ (unpaired *t*-test, $P = 0.047$). (**J**) Example traces of spontaneous release. (**K**) Spontaneous release amplitude is decreased in neurons rescued with $M18_{E59K}$ (unpaired *t*-test with Welch correction, $P = 0.016$). Decay time is comparable to control mEPSCs. (**L**) Cumulative frequency plot of spontaneous release events. Insert shows average frequency. (**M**) Neurons rescued with $M18_{E59K}$ show normal depression of EPSC size during repetitive stimulation at 10 Hz. Insets show the first three pulses and the average absolute amplitude of the first pulse. (**N**) An estimate of RRP size was made by back-extrapolation from the cumulative synchronous charge from the last 40 pulses within a 100-pulse train at 40 Hz. Inset shows average RRP sizes. No difference in RRP size was found.

of Syntaxin has a role beyond Munc18. Furthermore, the contribution of N-peptide binding can be different for different systems. For example, disrupting the N-peptide binding of UNC-18, unlike Munc18-1 (Burkhardt *et al*, 2008), also disrupted binding to monomeric Syntaxin (Johnson *et al*, 2009). It seems thus possible that in *C. elegans* the two binding sites cooperate much more strongly than in Munc18-1. Nevertheless, it needs to be tested by more rigorous biophysical methods like ITC whether the loss of the N-peptide entirely abolishes the binding of Syntaxin.

A number of recent studies using liposome fusion assays conclude that Munc18-1, like Sec1, promotes SNARE-dependent fusion and that binding the N-peptide is crucial in this respect (Shen *et al*, 2007; Rathore *et al*, 2010; Shen *et al*, 2010), probably by bringing Munc18-1 in close contact with the SNARE bundle (Diao *et al*, 2010; Rathore *et al*, 2010). *In vivo*, proximity between Munc18-1 and SNARE complexes could be achieved by additional factors or by Munc18-1 binding to closed Syntaxin, a step that most liposome fusion assays bypass by using liposomes with preassembled t-SNARE complexes. Indeed, a recent study revealed that Munc18-1 inhibits SNARE-mediated liposome fusion when the t-SNARE complex is not preassembled (Schollmeier *et al*, 2011), consistent with the well-established inhibitory effect of Munc18-1 on SNARE-complex formation *in vitro* (Pevsner *et al*, 1994b; Yang *et al*, 2000; Rickman *et al*, 2007; Burkhardt *et al*, 2008). Furthermore, stimulation of Munc18-1 in liposome fusion assays can only be observed after preincubation on ice with t-SNARE- and v-SNARE-containing liposomes and is limited to the beginning of the reaction. Therefore, it is conceivable that Munc18-1 promotes fusion by promoting SNARE assembly more than by acting on already assembled SNARE complexes. Furthermore, it was recently shown that purified squid Munc18-1 tends to aggregate in solution (Xu *et al*, 2011). This is consistent with our own observations on rat Munc18-1, which slowly aggregates and precipitates at higher concentrations (and also forced us to conduct binding experiments at concentrations lower than 20 μM in a previous study (Burkhardt *et al*, 2008). This tendency of Munc18 complicates standard liposome fusion assays due to potential light scattering artifacts and liposome clustering (Xu *et al*, 2011).

It has been known for a long time that Munc18-1 inhibits SNARE-complex formation *in vitro* (Pevsner *et al*, 1994a; Yang *et al*, 2000; Rickman *et al*, 2007; Burkhardt *et al*, 2008). Surprisingly, however, this aspect of Munc18's activity has not been studied much in the last years as it is often considered to be a peculiarity of the neuronal isoform that does not play a direct role in exocytosis. Nevertheless, the ability of choanoflagellate Munc18 to block SNARE assembly reveals that this feature of Munc18 is conserved and thus very likely must play an important role. Interestingly, although all mutants tested still bound with relatively high affinity to individual Syntaxin, the ability to control SNARE assembly was lost to a variable extent among the mutations described here, including one mutation, $M18_{E59K}$, which showed no inhibition at all (Figure 3E). Still all mutants supported transmission and no excess or aberrant fusion was observed. If anything, neurons rescued with $M18_{E59K}$ showed a slightly decreased Pr (Figure 3I). The reason that $M18_{E59K}$ is much more affected in its capacity for SNARE inhibition than the N-peptide mutants could be caused by the fast dissociation rate from monomeric Syntaxin1a (Figure 3D), a feature that could also be responsible for the reduced capacity of $M18_{E59K}$ to stimulate liposome fusion (Rodkey *et al*, 2008; Shen *et al*, 2010). Alternatively, binding of Munc18-1 to the SNARE complex might still have a subtle role on synaptic transmission, which for example might be reflected in the decreased Pr (increased PPR) of neurons rescued with $M18_{E59K}$. A similar trend can be observed in the N-terminal mutants, although we must stress that this cannot be seen as a true difference since statistical significance is not reached.

Taken together, recently published work and our own findings here suggest a revised model for the actions of Munc18-1 in exocytosis (Figure 4). As an initial step in the secretory pathway, Munc18 binds tightly to monomeric Syntaxin en route to the target membrane and probably sequesters individual Syntaxin molecules from larger multimers in the plasma membrane. As suggested by the crystal structure of both rat and choanoflagellate, Munc18-1 readily makes use of two binding sites in Syntaxin, the N-peptide and the remainder of the molecule in closed conformation. It is conceivable that in this complex, Munc18 establishes the

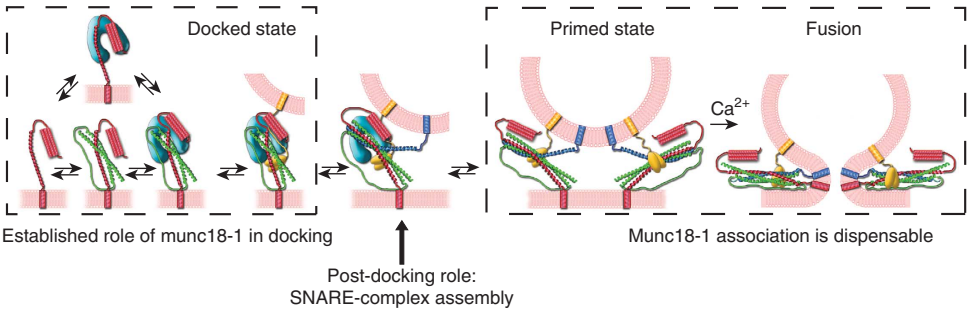

Figure 4 Schematic representation of the involvement of Munc18-1 in synaptic vesicle release. As an initial step in the secretory pathway, Munc18-1 (shown in cyan) binds tightly to monomeric Syntaxin (shown in red) via the N-peptide and the remainder of Syntaxin in closed conformation, probably sequestering individual Syntaxin molecules from larger multimers. Munc18 then establishes the right conformation and localization of Syntaxin to assemble into the acceptor complex (Syntaxin plus SNAP25 (shown in green)), which allows Synaptotagmin (shown in yellow) to bind to this acceptor complex and stably dock vesicles. This represents the established role of Munc18-1 in docking. Munc18-1 then assists Syntaxin in forming SNARE complexes, transferring vesicles from the docked state to the primed state. However, once the N-terminus of Synaptobrevin (shown in blue) associates to the Munc18/Syntaxin/SNAP25 complex to form a partially zippered, trans-SNARE complex and the vesicle is ready for Ca^{2+}-triggered fusion, Munc18–Syntaxin interactions are no longer required.

right conformation and localization of Syntaxin to assemble into the acceptor complex (Syntaxin plus SNAP25). This might allow synaptotagmin to bind to this acceptor complex and stably dock vesicles (de Wit *et al*, 2009). The Munc18/Syntaxin complex probably undergoes a conformational change during this process, which might be induced/controlled by other factors such as Munc13 and/or CAPS (Varoqueaux *et al*, 2002; Jockusch *et al*, 2007; Ma *et al*, 2011). Finally, the N-terminus of synaptobrevin associates to the Munc18/Syntaxin/SNAP25 complex to form a partially zippered, trans-SNARE complex, and might be supervised by other molecules such as complexin and synaptotagmin (see for a review (Walter *et al*, 2011)). In this situation, the vesicle is ready for Ca^{2+}-triggered fusion, which, according to our data, no longer requires Munc18–Syntaxin interactions. Hence, in this model, Munc18-1 does not need to dissociate from Syntaxin during SNARE assembly, but instead assists Syntaxin in forming SNARE complexes, but its association is dispensable once the N-terminus of synaptobrevin associates. Indeed, one study has shown that Munc18-1 dissociates from SNARE complexes in exchange for synaptobrevin association (Zilly *et al*, 2006). Alternatively, Munc18-1 stays attached and performs a role that is too subtle to be detected by the tools used in this study.

Notably, the docking defect in Munc18-1 knockout neurons can be rescued by SNAP25 overexpression, although secretion remains arrested (de Wit *et al*, 2009). This observation suggests that Munc18, in addition to its established role in docking, also has a role in the following steps. The data in our current study position this post-docking role at the step(s) before the SNARE complex is fully assembled, that is, during association of the N-terminus of synaptobrevin with the Syntaxin:SNAP25 acceptor complex. At this stage, SM proteins may no longer be required and their continued association to assembled SNARE complexes is dispensable.

Materials and methods

Munc18-1-deficient mice

Munc18-1-deficient mice were generated as described previously (Verhage *et al*, 2000). Munc18-1 null mutant mice are stillborn and can be easily distinguished from wild-type or heterozygous littermates. E18 embryos were obtained by caesarian section of pregnant females from timed heterozygous mating. Animals were housed and bred according to the Institutional, Dutch and US governmental guidelines.

Constructs

We substituted leucine L130 for lysine or phenylalanine F115 for glutamic acid by subcloning the fragments in PCRblunt (Invitrogen) to create $M18_{L130K}$ and $M18_{F115E}$, respectively. $M18_{WT}$, $M18_{L130K}$ and $M18_{F115E}$ were cloned into pIRES$_2$EGFP (Clontech). $M18_{E59K}$ was created from $M18_{WT}$IRES$_2$EGFP by substituting glutamic acid E59 for lysine using Quickchange (Stratagene). All constructs were subcloned into pLenti vectors, and viral particles were produced as described (Naldini *et al*, 1996). Transduction efficiencies were assessed on HEK cells and taken into account when applied to rescue neuronal cultures.

Protein expression and purification

The bacterial expression constructs for SNARE proteins, cysteine-free SNAP-25A (1–206), the soluble portion of Syntaxin1a (1–262) and the soluble portion of Synaptobrevin 2 (1–96) have been described before. Likewise, the single-cysteine SNARE protein variants used for labelling Syb2 Cys79 has been published (Burkhardt *et al*, 2008). Full-length Munc18-1 and the three Munc18-1 mutants L130K, F115E and E59K were constructed by site-directed mutagenesis. All constructs were cloned into a pET28a vector and expressed in *E. coli*. Proteins and SNARE complexes assembled from purified monomers were purified by Ni^{2+}-NTA affinity chromatography followed by ion-exchange chromatography essentially as described (Burkhardt *et al*, 2008).

Isothermal titration calorimetry

ITC was performed on a VP-ITC instrument (GE Healthcare) at 25 °C. Samples were dialyzed against degassed PBS buffer (20 mM sodium phosphate, pH 7.4, 150 mM NaCl and 1 mM DTT). Titrations were carried out by 20 μl injections. The measured heat released upon binding was integrated and analysed with Microcal Origin 7.0 using a single-site binding model, yielding the equilibrium association constant *Ka*, the enthalpy of binding ΔH and the stoichiometry *N*. Experimental data are shown in Supplementary Figure S1.

Fluorescence spectroscopy

Fluorescence measurements were carried out in a Fluorolog 3 spectrometer in T-configuration equipped for polarization (Horiba Scientific). Single-cysteine variants were labelled with Texas Red C5 bromoacetamide or Oregon Green 488 iodoacetamide according to the manufacturer's instructions (Invitrogen). All experiments were performed at 25 °C in 1-cm quartz cuvettes in PBS buffer. Fluorescence anisotropy, which is used to indicate the local flexibility of the labelled residue, and which increases upon complex formation and decreases upon dissociation, was measured essentially as described (Burkhardt *et al*, 2008). The *G* factor was calculated according to $G = I_{HV}/I_{HH}$, where *I* is the fluorescence intensity, and the first subscript letter indicates the direction of the exciting light and the second subscript letter the direction of emitted light. The intensities of the vertically (V) and horizontally (H) polarized emission light after excitation by vertically polarized light were measured. The anisotropy (*r*) was determined according to $r = (I_{VV} - GI_{VH})/(I_{VV} + 2GI_{VH})$. During competitive dissociation experiments, an excess of unlabelled $Syx1a_{1-262}$ (5 μM) was added to a premix of 100-nM Oregon Green-labelled $Syx1a_{1-262}$ and 200 nM Munc18, and the decrease in fluorescence anisotropy measured. The dissociation was fitted by a single exponential fit. Ternary SNARE-complex formation was followed by the increase in fluorescence anisotropy of labelled $Syb2_{1-96}$ (40 nM) upon mixing with 500 nM Syntaxin1a and 750 nM SNAP25 in the absence or presence of 750 nM Munc18-1.

Neuronal cultures

Hippocampi and cortices were separately collected in ice-cold Hanks Buffered Salt Solution (HBSS; Sigma) buffered with 7 mM HEPES (Invitrogen). After removal of the meninges, neurons were incubated in Hanks-HEPES with 0.25% trypsin (Invitrogen) for 20 min at 37 °C. After washing, neurons were triturated and counted in a Fuchs–Rosenthal chamber. Neurons were plated in prewarmed Neurobasal medium (Invitrogen) supplemented with 2% B-27 (Invitrogen), 1.8% HEPES, 0.25% glutamax (Invitrogen) and 0.1% Pen/Strep (Invitrogen). To achieve autaptic cultures, hippocampal neurons were plated at a density of 6 K/well of a 12-well plate on microislands of rat glia. These microislands were generated by plating 8 K/well rat glia on UV-sterilized agarose-coated etched glass coverslips stamped with a 0.1 mg/ml poly-D-lysine (Sigma) and 0.2 mg/ml rat tail collagen (BD Biosciences) solution. Network cultures were generated by plating cortical neurons (100–500 K/well on a 12-well plate) on a confluent layer of rat glia grown on etched glass coverslips sprayed with a 0.1 mg/ml poly-D-lysine and 0.2 mg/ml rat tail collagen (BD Biosciences) solution. Neurons were infected at DIV0 with lentiviral particles encoding $M18_{WT}$, $M18_{L130K}$, $M18_{F115E}$ and $M18_{E59K}$, and were allowed to develop for 13–18 days before measuring. For protein level measurements, neurons were plated at 100 K/well in a 12-well plate containing etched glass coverslips coated with 0.5 milli-percent poly-L-ornithine (Sigma) and 2 μg/ml laminin (Sigma), and were grown for 10–11 days before fixation.

Electrophysiological recordings

Whole-cell voltage-clamp recordings ($Vm = -70$ mV) were performed on autaptic or network cultures on DIV 13–18 at room temperature. External solution contained the following (in mM): 10 HEPES, 10 glucose, 140 NaCl, 2.4 KCl, 4 $MgCl_2$ and 4 $CaCl_2$

(pH = 7.30, 300 mOsmol). Gabazine (Sigma) was added to the external solution at a concentration of 20 μM to isolate excitatory currents. Patch-pipette solution contained the following (in mM): 125 K^+–gluconic acid, 10 NaCl, 4.6 $MgCl_2$, 15 creatine phosphate, 10 U/ml phosphocreatine kinase and 1 EGTA (pH 7.30). Recordings were performed with an Axopatch 200A amplifier (Molecular Devices). Digidata 1322A and Clampex 9.0 (Molecular Devices) were used for signal acquisition. After whole-cell mode was established, only cells with an access resistance of $<12\,M\Omega$ and leak current of <500 pA were accepted for analysis. In autaptic neurons, EPSCs were elicited by a 0.5 ms depolarization to 30 mV. Responses below 300 pA were excluded from analysis. The percentage of excluded cells was similar for all groups except for $M18_{E59K}$ rescued neurons ($M18_{WT}$, 24%; $M18_{L130K}$, 29%; $M18_{F115E}$, 28%; $M18_{E59K}$, 48% of cells excluded). Local field stimulation (1 mA, 1 ms) was applied with a bipolar concentric electrode placed in the vicinity of the patched neuron. Spontaneous release in networks was measured in the presence of 1 μM tetrodotoxin (Ascent) to block Na^+ currents. Offline analysis of electrophysiology was performed using Clampfit v9.0 (Axon Instruments), Mini Analysis Program v6.0 (synaptosoft) and custom-written software routines in Matlab 7.1 or R2009b (Mathworks).

Immunocytochemistry

Cultures were fixed with 3.7% formaldehyde (Electron Microscopy Sciences). After washing with PBS, cells were permeated with 0.1% Triton X-100 for 5 min and incubated in 2% normal goat serum for 20 min to block aspecific binding. Cells were incubated for 1 h at room temperature in a mixture of monoclonal mouse anti-VAMP (1:1000, SySy), polyclonal chicken anti-MAP2 (1:10 000, Abcam) and polyclonal rabbit anti-Munc18-1 (1:500, SySy) antibodies. After washing, cells were incubated for 1 h at room temperature with second antibodies conjugated to Alexa dyes (1:1000, Molecular Probes) and washed again. Coverslips were mounted with Mowiol-Dabco and imaged with a confocal LSM510 microscope (Carl Zeiss) using a $\times 40$ oil immersion objective with $\times 0.7$ zoom at 1024×1024 pixels. Neuronal morphology and protein levels were analysed using a published automated image analysis routine (Schmitz *et al*, 2011).

Electron microscopy

Autaptic hippocampal cultures of munc18-1 null mutant mice (E18) obtained from two different litters were fixed at DIV14-16 for 45 min at room temperature with 2.5% glutaraldehyde in 0.1 M cacodylate buffer (pH 7.4) (de Wit *et al*, 2006; Wierda *et al*, 2007). As for electrophysiology, only glia islands containing a single neuron were used for analysis. After fixation, cells were washed three times for 5 min with 0.1 M cacodylate buffer (pH 7.4), post-fixed for 2 h at room temperature with 1% Osmium tetroxide/1% potassium ferrocyanide in bidest, washed and stained with 1% uranyl acetate for 40 min in the dark. Following dehydration through a series of increasing ethanol concentrations, cells were embedded in Epon and polymerized for 24 h at 60 °C. After polymerization of the Epon, the coverslip was removed by alternately dipping it in liquid nitrogen and hot water. Cells of interest were selected by observing the flat Epon-embedded cell monolayer under the light microscope, and mounted on prepolymerized Epon blocks for thin sectioning. Ultrathin sections (~90 nm) were cut parallel to the cell monolayer and collected on single-slot, formvar-coated copper grids, and stained in uranyl acetate and lead citrate. Autaptic synapses were selected at low magnification using a JEOL 1010 electron microscope. All analyses were performed on single ultrathin sections of randomly selected synapses. The distribution of synaptic vesicles, total synaptic vesicle number and active zone length were measured with Image J (National Institute of Health, USA) on digital images of synapses taken at $\times 100\,000$ magnification using analySIS software (Soft Imaging System, Gmbh, Germany). The observer was blinded for the genotype. For all morphological analyses, we selected only synapses with intact synaptic plasma membranes with a recognizable pre- and postsynaptic density and clear synaptic vesicle membranes. Docked synaptic vesicles had a distance of 0 nm from the synaptic vesicle membrane to the active zone membrane. The active zone membrane was recognized as a specialized part of the presynaptic plasma membrane that contained a clear presynaptic density. To get an estimate size of the total synaptic vesicle pool, distances of undocked synaptic vesicles to the active zone membrane were also included in our measurements.

Data analysis

Data are presented as mean values ± s.e.m., with n referring to the number of cells from each group. Statistical analysis was performed with Instat v3.05 software (GraphPad Software). Data samples were first tested for normality with the Kolmogorov and Smirnov test, and for heterogeneity of variance with the method of Bartlett. If data allowed an unpaired t-test (Welch correction was adopted when variances were unequal) or an ANOVA was used to determine statistical significance. Alternatively, the nonparametric Mann–Whitney U-test or the Kruskal–Wallis Test (for comparing one or multiple groups, respectively) was used. If a test for multiple groups reached significance, post-testing to compare the experimental to the control group was performed using the parametric Bonferroni post-test or the nonparametric Dunn's post-test. P-values below 0.05 are considered significant and are indicated by asterisks ($^*P<0.05$, $^{**}P<0.01$ and $^{***}P<0.001$).

Supplementary data

Supplementary data are available at *The EMBO Journal* Online (http://www.embojournal.org).

Acknowledgements

We thank R Zalm, D Schut, I Saarloos, J Hoetjes, B Beuger, H Lodder and J Wortel for technical assistance, and C van der Meer, B Tersteeg and M Boin for animal breeding and maintenance. R Dekker is acknowledged for excellent electron microscopical analyses. This work was supported by the EU (EUSynapse project 019055 to MV, EUROSPIN project HEALTH-F2-2009-241498 to MV and HEALTH-F2-2009-242167 SynSys project to MV), the Netherlands Organization for Scientific Research, NWO (Pionier/VICI 900-01-001 and ZonMW 903-42-095 to MV; and VENI 916-36-043 to HdW) and the NeuroBsik Mouse Phenomics Consortium (BSIK03053).

Author contributions: MM and PB performed most of the experiments, and analysed and interpreted the data. HdW contributed to the EM data. MV, DF and RFT conceived–designed the project and interpreted the results. MM, MV and DF wrote the manuscript with inputs from all authors.

Conflict of interest

The authors declare that they have no conflict of interest.

References

Brandie FM, Aran V, Verma A, McNew JA, Bryant NJ, Gould GW (2008) Negative regulation of syntaxin4/SNAP-23/VAMP2-mediated membrane fusion by Munc18c *in vitro*. *PLoS ONE* **3:** e4074

Burgoyne RD, Barclay JW, Ciufo LF, Graham ME, Handley MT, Morgan A (2009) The functions of Munc18-1 in regulated exocytosis. *Ann N Y Acad Sci* **1152:** 76–86

Burkhardt P, Hattendorf DA, Weis WI, Fasshauer D (2008) Munc18a controls SNARE assembly through its interaction with the syntaxin N-peptide. *EMBO J* **27:** 923–933

Burkhardt P, Stegmann CM, Cooper B, Kloepper TH, Imig C, Varoqueaux F, Wahl MC, Fasshauer D (2011) Primordial neurosecretory apparatus identified in the choanoflagellate Monosiga brevicollis. *Proc Natl Acad Sci USA* **108:** 15264–15269

Carpp LN, Ciufo LF, Shanks SG, Boyd A, Bryant NJ (2006) The Sec1p/Munc18 protein Vps45p binds its cognate SNARE proteins via two distinct modes. *J Cell Biol* **173:** 927–936

Carr CM, Grote E, Munson M, Hughson FM, Novick PJ (1999) Sec1p binds to SNARE complexes and concentrates at sites of secretion. *J Cell Biol* **146:** 333–344

Carr CM, Rizo J (2010) At the junction of SNARE and SM protein function. *Curr Opin Cell Biol* **22:** 488–495

de Wit H, Cornelisse LN, Toonen RF, Verhage M (2006) Docking of secretory vesicles is syntaxin dependent. *PLoS ONE* **1:** e126

de Wit H, Walter AM, Milosevic I, Gulyas-Kovacs A, Riedel D, Sorensen JB, Verhage M (2009) Synaptotagmin-1 docks secretory vesicles to syntaxin-1/SNAP-25 acceptor complexes. *Cell* **138:** 935–946

Deak F, Xu Y, Chang WP, Dulubova I, Khvotchev M, Liu X, Sudhof TC, Rizo J (2009) Munc18-1 binding to the neuronal SNARE complex controls synaptic vesicle priming. *J Cell Biol* **184:** 751–764

Diao J, Su Z, Lu X, Yoon TY, Shin YK, Ha T (2010) Single-vesicle fusion assay reveals Munc18-1 binding to the SNARE core is sufficient for stimulating membrane fusion. *ACS Chem Neurosci* **1:** 168–174

Dulubova I, Khvotchev M, Liu S, Huryeva I, Sudhof TC, Rizo J (2007) Munc18-1 binds directly to the neuronal SNARE complex. *Proc Natl Acad Sci USA* **104:** 2697–2702

Dulubova I, Sugita S, Hill S, Hosaka M, Fernandez I, Sudhof TC, Rizo J (1999) A conformational switch in syntaxin during exocytosis: role of munc18. *EMBO J* **18:** 4372–4382

Dulubova I, Yamaguchi T, Arac D, Li H, Huryeva I, Min SW, Rizo J, Sudhof TC (2003) Convergence and divergence in the mechanism of SNARE binding by Sec1/Munc18-like proteins. *Proc Natl Acad Sci USA* **100:** 32–37

Fisher RJ, Pevsner J, Burgoyne RD (2001) Control of fusion pore dynamics during exocytosis by Munc18. *Science (New York, NY* **291:** 875–878

Graham ME, Barclay JW, Burgoyne RD (2004) Syntaxin/Munc18 interactions in the late events during vesicle fusion and release in exocytosis. *J Biol Chem* **279:** 32751–32760

Guan R, Dai H, Rizo J (2008) Binding of the Munc13-1 MUN domain to membrane-anchored SNARE complexes. *Biochemistry* **47:** 1474–1481

Gulyas-Kovacs A, de Wit H, Milosevic I, Kochubey O, Toonen R, Klingauf J, Verhage M, Sorensen JB (2007) Munc18-1: sequential interactions with the fusion machinery stimulate vesicle docking and priming. *J Neurosci* **27:** 8676–8686

Han GA, Malintan NT, Collins BM, Meunier FA, Sugita S (2010) Munc18-1 as a key regulator of neurosecretion. *J Neurochem* **115:** 1–10

Han GA, Malintan NT, Saw NM, Li L, Han L, Meunier FA, Collins BM, Sugita S (2011) Munc18-1 domain-1 controls vesicle docking and secretion by interacting with syntaxin-1 and chaperoning it to the plasma membrane. *Mol Biol Cell* **22:** 4134–4149

Harrison SD, Broadie K, van de Goor J, Rubin GM (1994) Mutations in the Drosophila Rop gene suggest a function in general secretion and synaptic transmission. *Neuron* **13:** 555–566

Hashizume K, Cheng YS, Hutton JL, Chiu CH, Carr CM (2009) Yeast Sec1p functions before and after vesicle docking. *Mol Biol Cell* **20:** 4673–4685

Hata Y, Slaughter CA, Sudhof TC (1993) Synaptic vesicle fusion complex contains unc-18 homologue bound to syntaxin. *Nature* **366:** 347–351

Jockusch WJ, Speidel D, Sigler A, Sorensen JB, Varoqueaux F, Rhee JS, Brose N (2007) CAPS-1 and CAPS-2 are essential synaptic vesicle priming proteins. *Cell* **131:** 796–808

Johnson JR, Ferdek P, Lian LY, Barclay JW, Burgoyne RD, Morgan A (2009) Binding of UNC-18 to the N-terminus of syntaxin is essential for neurotransmission in caenorhabditis elegans. *Biochem J* **418:** 73–80

Jorgacevski J, Potokar M, Grilc S, Kreft M, Liu W, Barclay JW, Buckers J, Medda R, Hell SW, Parpura V, Burgoyne RD, Zorec R (2011) Munc18-1 tuning of vesicle merger and fusion pore properties. *J Neurosci* **31:** 9055–9066

Khvotchev M, Dulubova I, Sun J, Dai H, Rizo J, Sudhof TC (2007) Dual modes of Munc18-1/SNARE interactions are coupled by functionally critical binding to syntaxin-1 N terminus. *J Neurosci* **27:** 12147–12155

Latham CF, Lopez JA, Hu SH, Gee CL, Westbury E, Blair DH, Armishaw CJ, Alewood PF, Bryant NJ, James DE, Martin JL (2006) Molecular dissection of the Munc18c/syntaxin4 interaction: implications for regulation of membrane trafficking. *Traffic (Copenhagen, Denmark)* **7:** 1408–1419

Ma C, Li W, Xu Y, Rizo J (2011) Munc13 mediates the transition from the closed syntaxin-Munc18 complex to the SNARE complex. *Nat Struct Mol Biol* **18:** 542–549

Malintan NT, Nguyen TH, Han L, Latham CF, Osborne SL, Wen PJ, Lim SJ, Sugita S, Collins BM, Meunier FA (2009) Abrogating Munc18-1-SNARE complex interaction has limited impact on exocytosis in PC12 cells. *J Biol Chem* **284:** 21637–21646

McEwen JM, Kaplan JM (2008) UNC-18 promotes both the anterograde trafficking and synaptic function of syntaxin. *Mol Biol Cell* **19:** 3836–3846

Misura KM, Scheller RH, Weis WI (2000) Three-dimensional structure of the neuronal-Sec1-syntaxin 1a complex. *Nature* **404:** 355–362

Naldini L, Blomer U, Gallay P, Ory D, Mulligan R, Gage FH, Verma IM, Trono D (1996) *In vivo* gene delivery and stable transduction of nondividing cells by a lentiviral vector. *Science (New York, NY* **272:** 263–267

Peng R, Gallwitz D (2004) Multiple SNARE interactions of an SM protein: Sed5p/Sly1p binding is dispensable for transport. *EMBO J* **23:** 3939–3949

Pevsner J, Hsu SC, Braun JE, Calakos N, Ting AE, Bennett MK, Scheller RH (1994a) Specificity and regulation of a synaptic vesicle docking complex. *Neuron* **13:** 353–361

Pevsner J, Hsu SC, Scheller RH (1994b) n-Sec1: a neural-specific syntaxin-binding protein. *Proc Natl Acad Sci USA* **91:** 1445–1449

Pieren M, Schmidt A, Mayer A (2010) The SM protein Vps33 and the t-SNARE H(abc) domain promote fusion pore opening. *Nat Struct Mol Biol* **17:** 710–717

Rathore SS, Bend EG, Yu H, Hammarlund M, Jorgensen EM, Shen J (2010) Syntaxin N-terminal peptide motif is an initiation factor for the assembly of the SNARE-Sec1/Munc18 membrane fusion complex. *Proc Natl Acad Sci USA* **107:** 22399–22406

Rickman C, Medine CN, Bergmann A, Duncan RR (2007) Functionally and spatially distinct modes of munc18-syntaxin 1 interaction. *J Biol Chem* **282:** 12097–12103

Rodkey TL, Liu S, Barry M, McNew JA (2008) Munc18a scaffolds SNARE assembly to promote membrane fusion. *Mol Biol Cell* **19:** 5422–5434

Schmitz SK, Hjorth JJ, Joemai RM, Wijntjes R, Eijgenraam S, de Bruijn P, Georgiou C, de Jong AP, van Ooyen A, Verhage M, Cornelisse LN, Toonen RF, Veldkamp WJ (2011) Automated analysis of neuronal morphology, synapse number and synaptic recruitment. *J Neurosci Methods* **195:** 185–193

Schneggenburger R, Meyer AC, Neher E (1999) Released fraction and total size of a pool of immediately available transmitter quanta at a calyx synapse. *Neuron* **23:** 399–409

Schollmeier Y, Krause JM, Kreye S, Malsam J, Sollner T (2011) Resolving the function of distinct Munc18-1-SNARE interaction modes in a reconstituted membrane fusion assay. *J Biol Chem* **286:** 30582–30590

Scott BL, Van Komen JS, Irshad H, Liu S, Wilson KA, McNew JA (2004) Sec1p directly stimulates SNARE-mediated membrane fusion *in vitro*. *J Cell Biol* **167:** 75–85

Shen J, Rathore SS, Khandan L, Rothman JE (2010) SNARE bundle and syntaxin N-peptide constitute a minimal complement for Munc18-1 activation of membrane fusion. *J Cell Biol* **190:** 55–63

Shen J, Tareste DC, Paumet F, Rothman JE, Melia TJ (2007) Selective activation of cognate SNAREpins by Sec1/Munc18 proteins. *Cell* **128:** 183–195

Smyth AM, Duncan RR, Rickman C (2010) Munc18-1 and syntaxin1: unraveling the interactions between the dynamic duo. *Cellular Mol Neurobiol* **30:** 1309–1313

Sudhof TC, Rothman JE (2009) Membrane fusion: grappling with SNARE and SM proteins. *Science (New York, NY* **323:** 474–477

Togneri J, Cheng YS, Munson M, Hughson FM, Carr CM (2006) Specific SNARE complex binding mode of the Sec1/Munc-18 protein, Sec1p. *Proc Natl Acad Sci USA* **103:** 17730–17735

Toonen RF, Kochubey O, de Wit H, Gulyas-Kovacs A, Konijnenburg B, Sorensen JB, Klingauf J, Verhage M (2006a) Dissecting docking and tethering of secretory vesicles at the target membrane. *EMBO J* **25:** 3725–3737

Toonen RF, Verhage M (2003) Vesicle trafficking: pleasure and pain from SM genes. *Trends Cell Biol* **13:** 177–186

Toonen RF, Verhage M (2007) Munc18-1 in secretion: lonely Munc joins SNARE team and takes control. *Trends Neurosci* **30:** 564–572

Toonen RF, Wierda K, Sons MS, de Wit H, Cornelisse LN, Brussaard A, Plomp JJ, Verhage M (2006b) Munc18-1 expression levels control synapse recovery by regulating readily releasable pool size. *Proc Natl Acad Sci USA* **103:** 18332–18337

Varoqueaux F, Sigler A, Rhee JS, Brose N, Enk C, Reim K, Rosenmund C (2002) Total arrest of spontaneous and evoked synaptic transmission but normal synaptogenesis in the absence of Munc13-mediated vesicle priming. *Proc Natl Acad Sci USA* **99:** 9037–9042

Verhage M, Maia AS, Plomp JJ, Brussaard AB, Heeroma JH, Vermeer H, Toonen RF, Hammer RE, van den Berg TK, Missler M, Geuze HJ, Sudhof TC (2000) Synaptic assembly of the brain in the absence of neurotransmitter secretion. *Science (New York, NY* **287:** 864–869

Verhage M, Sorensen JB (2008) Vesicle docking in regulated exocytosis. *Traffic (Copenhagen, Denmark)* **9:** 1414–1424

Voets T, Toonen RF, Brian EC, de Wit H, Moser T, Rettig J, Sudhof TC, Neher E, Verhage M (2001) Munc18-1 promotes large dense-core vesicle docking. *Neuron* **31:** 581–591

Walter AM, Groffen AJ, Sorensen JB, Verhage M (2011) Multiple Ca(2+) sensors in secretion: teammates, competitors or autocrats? *Trends Neurosci* **34:** 487–497

Weber-Boyvat M, Aro N, Chernov KG, Nyman T, Jantti J (2011) Sec1p and Mso1p C-terminal tails cooperate with the SNAREs and Sec4p in polarized exocytosis. *Mol Biol Cell* **22:** 230–244

Weimer RM, Richmond JE, Davis WS, Hadwiger G, Nonet ML, Jorgensen EM (2003) Defects in synaptic vesicle docking in unc-18 mutants. *Nat Neurosci* **6:** 1023–1030

Weninger K, Bowen ME, Choi UB, Chu S, Brunger AT (2008) Accessory proteins stabilize the acceptor complex for synaptobrevin, the 1:1 syntaxin/SNAP-25 complex. *Structure* **16:** 308–320

Wierda KD, Toonen RF, de Wit H, Brussaard AB, Verhage M (2007) Interdependence of PKC-dependent and PKC-independent pathways for presynaptic plasticity. *Neuron* **54:** 275–290

Williams AL, Ehm S, Jacobson NC, Xu D, Hay JC (2004) rsly1 binding to syntaxin 5 is required for endoplasmic reticulum-to-Golgi transport but does not promote SNARE motif accessibility. *Mol Biol Cell* **15:** 162–175

Xu Y, Seven AB, Su L, Jiang QX, Rizo J (2011) Membrane bridging and hemifusion by denaturated munc18. *PLoS ONE* **6:** e22012

Xu Y, Su L, Rizo J (2010) Binding of Munc18-1 to synaptobrevin and to the SNARE four-helix bundle. *Biochemistry* **49:** 1568–1576

Yamaguchi T, Dulubova I, Min SW, Chen X, Rizo J, Sudhof TC (2002) Sly1 binds to Golgi and ER syntaxins via a conserved N-terminal peptide motif. *Dev Cell* **2:** 295–305

Yang B, Steegmaier M, Gonzalez Jr. LC, Scheller RH (2000) nSec1 binds a closed conformation of syntaxin1A. *J Cell Biol* **148:** 247–252

Zilly FE, Sorensen JB, Jahn R, Lang T (2006) Munc18-bound syntaxin readily forms SNARE complexes with synaptobrevin in native plasma membranes. *PLoS Biol* **4:** e330

